Channels 3:5, 1-6; September/October 2009; © 2009 Landes Bioscience

Characterization of the calmodulin-binding site in the N terminus of $Ca_V1.2$

Adva Benmocha,[1,*] Lior Almagor,[2] Shimrit Oz,[1] Joel A. Hirsch[2] and Nathan Dascal[1,*]

[1]Department of Physiology and Pharmacology; Sackler School of Medicine; [2]Department of Biochemistry; George S. Weiss Faculty of Life Sciences; Tel Aviv University; Tel Aviv, Israel

Keywords: calcium channel, L-type, $Ca_V1.2$, calmodulin, binding, inactivation

Abbreviations: CaM, calmodulin; CDI, calcium-dependent inactivation; CT, C-terminus; NSCaTE, N-terminal spatial Ca^{2+} transforming element; NT, N-terminus; VDI, voltage-dependent inactivation

Interaction of calmodulin (CaM) with the C-terminus (CT) of the L-type $Ca_V1.2$ channel is crucial for Ca^{2+}-dependent inactivation (CDI). CaM also binds to the N-terminus (NT), and a CaM-formed "bridge" between CT and NT has been proposed to control CDI. We characterized the interaction of CaM with its NT-binding peptide. Binding is Ca^{2+}-dependent with an affinity of 0.6 μM. Mutations in NT of $Ca_V1.2$ that abolished the binding of CaM only slightly weakened the CDI but also accelerated the VDI. CaM did not foster an interaction between the CaM-binding peptides of NT and CT. Thus, the role of CaM's interaction with the $Ca_V1.2$ NT remains to be determined.

Introduction

$Ca_V1.2$ is a voltage-dependent Ca^{2+} channel (VDCC) of the L-type, present in cardiac and smooth muscle, endocrine cells and neurons, which produces calcium influx in response to membrane depolarization. Inactivation, loss of conductance during stimulation, is an important negative feedback mechanism in which VDCCs are regulated by internal Ca^{2+} levels (Ca^{2+}-dependent inactivation, CDI) and membrane potential (voltage-dependent inactivation, VDI), producing short and accurate Ca^{2+} signals.[1] The physiological mechanism of inactivation is incompletely understood, and it is unclear whether the CDI and the VDI use different structural determinants or identical ones (reviewed in ref. 2). Inactivation is affected by auxiliary β subunits and by multiple regions in the main, pore forming subunit of $Ca_V1.2$ (α_{1C}), among them its cytosolic N and C termini (NT and CT) which serve as scaffolds for various signaling molecules, including calmodulin (CaM).[3-7]

CaM is a soluble, 17 kDa Ca^{2+}-binding protein which serves as a critical Ca^{2+} sensor of many VDCCs. It is involved in two different types of regulation: CDI and CDF (Ca^{2+} dependent facilitation).[4,8] CaM consists of 2 lobes. In most VDCCs, the C-lobe of CaM, which binds Ca^{2+} with a higher affinity than the N-lobe,[9] underlies the channel's sensitivity to fast changes in the "local" Ca^{2+} in the nano-domain (immediate vicinity) of the channel and triggers a rapid CDI process, whereas the N-lobe senses the slower, distributed intracellular ("global") Ca^{2+} rises from more remote sources and initiates a more gradual and distinct CDI mechanism.[3,10]

CaM interacts with multiple sites in α_{1C}, of which the C-terminal pre-IQ and IQ domains are best characterized;[11] mutations in these CaM binding sites abolish CDI. In the IQ domain alone, it has a high affinity binding site for the C-lobe of CaM (K_D of 2.63 nM), an overlapping intermediate affinity binding site for the N-lobe of CaM (K_D of 57.6 nM), and a separate low affinity binding site for the N-lobe of CaM (K_D of 19.2 μM), upstream to the high-affinity binding sites.[12] CaM is permanently anchored to the CT in a Ca^{2+}-independent manner, and elevation of Ca^{2+} causes rearrangements among CaM and its CT-binding sites.[13,14] CaM also binds to the NT[5] and the exact location of CaM binding site in the NT has been identified recently.[15] This N-lobe CaM regulation site, termed NSCaTE (N Terminal Spatial Ca^{2+} Transforming Element), exists in the L-type channels $Ca_V1.2$ and $Ca_V1.3$ but not in other VDCCs such as $Ca_V2.2$. Transfer of NSCaTE to $Ca_V2.2$ renders the channel's CDI more robust and less sensitive to Ca^{2+} chelation.[15] However, the role of the N-terminal CaM binding site in $Ca_V1.2$ itself is unclear. In $Ca_V1.2$, CDI is robust and highly sensitive to nano-domain Ca^{2+}. Since the binding of CaM to the NT is strictly Ca^{2+}-dependent,[5] it has been hypothesized that, following Ca^{2+} entry via the channel, the previously CT-anchored CaM also binds the NT, forming an NT-CT "bridge" that is important for CDI.[5,15] In this study, we characterized the interaction between CaM and a CaM-binding NT peptide and examined the involvement of NSCaTE and the putative NT-CT bridge in CDI of the $Ca_V1.2$ channel.

Results

CaM has a Ca^{2+}-dependent, medium-affinity binding site in the NT of $Ca_V1.2$. Pull-down experiments with GST-fusions of α_{1C} NT (**Fig. 1A**, left) showed that GST-NT_{60-100} and GST-NT_{60-120} but not GST-NT_{1-60} and GST-NT_{95-154} proteins,

*Correspondence to: Adva Benmocha and Nathan Dascal; Email: advabne@post.tau.ac.il and dascaln@post.tau.ac.il
Submitted: 07/01/09; Revised: 07/17/09; Accepted: 07/29/09
Previously published online: www.landesbioscience.com/journals/Channels/9686

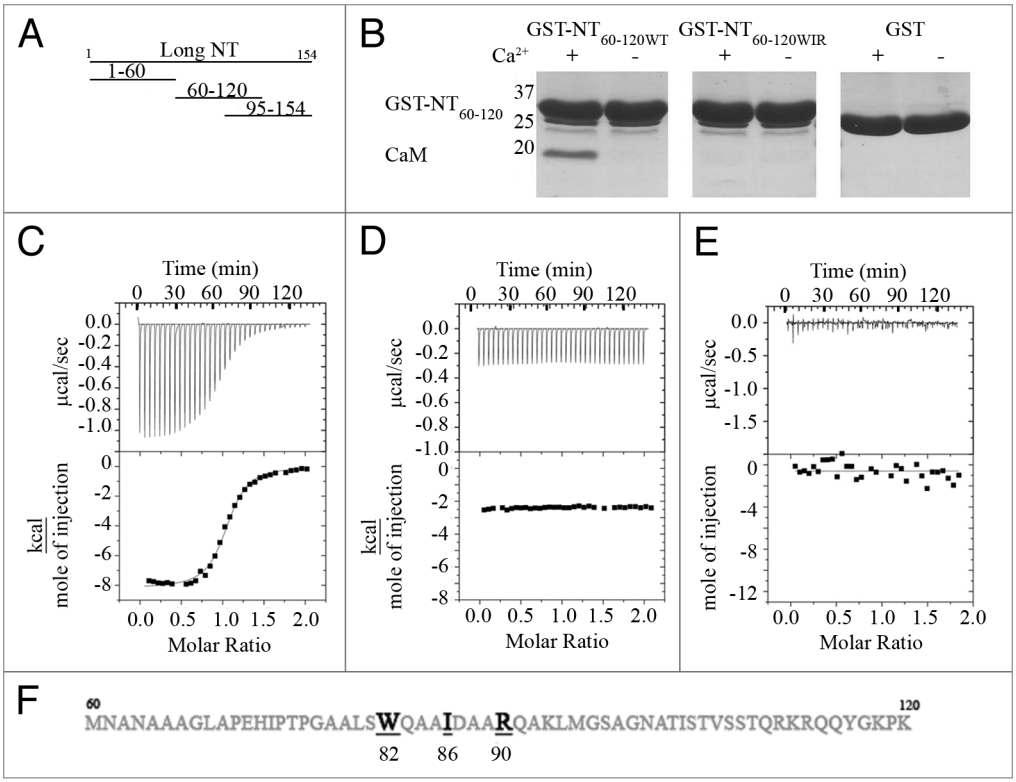

Figure 1. CaM has a Ca^{2+}-dependent medium affinity binding site in the NT of $Ca_V1.2$. (A) Schematic presentation of GST-fused proteins of the NT of α_{1C}. (B) Interaction of GST-$NT_{60\text{-}120WT}$ (left), GST-$NT_{60\text{-}120WIR}$ (middle) and GST (right) with CaM in the presence of 1 mM Ca^{2+} or 1 mM EGTA (no Ca^{2+}). Equimolar amounts of all proteins (10 µM) were used. The experiment was done in binding buffer with 0.5% CHAPS. Proteins were stained with Coomassie Blue. (C) ITC characterization of Ca^{2+}-CaM interaction with $NT_{60\text{-}120}$. 419.5 µM of CaM was injected into the ITC cell containing 42 µM $NT_{60\text{-}120}$, in a buffer containing 2 mM Ca^{2+}. Top, 8 µl injections of CaM into the cell. Bottom, binding isotherms. This is a representative experiment out of three. (D) ITC characterization of CaM interaction with $NT_{60\text{-}120}$. 419.5 µM of CaM was injected into the ITC cell containing 38 µM $NT_{60\text{-}120}$, in buffer containing 2 mM EGTA. Top, 8 µl injections of CaM into the cell. Bottom, binding isotherms. (E) ITC characterization of Ca^{2+}-CaM interaction with GST-$NT_{60\text{-}120WIR}$. 346 µM of CaM was injected into the ITC cell containing 38 µM GST-$NT_{60\text{-}120WIR}$, in buffer containing 1 mM Ca^{2+}. Top, 8 µl injections of CaM into the cell. Bottom, binding isotherms. This is a representative experiment out of 2. (F) Amino acid sequence of $NT_{60\text{-}120}$. The a.a. mutated for the WIR mutation are in bold.

bound in vitro translated CaM (data not shown). The location of the CaM-binding site determined in this study by pull-down is in full agreement with the functional and fluorescence resonance transfer (FRET)-based mapping of NSCaTE to amino acids (a.a.) 80–94 by Dick et al.[15]

GST-$NT_{60\text{-}120}$, but not GST (right), bound purified recombinant CaM in the presence of Ca^{2+} but not in a Ca^{2+}-free, EGTA-containing buffer. Quantitative characterization of CaM binding to its NT site was performed with $NT_{60\text{-}120}$ (without GST) using isothermal titration calorimetry (ITC) (**Fig. 1B**). The equilibrium binding constant (Kb) was found to be $1.75 \times 10^6 \pm 1.12 \times 10^5$ M^{-1} (corresponding to a dissociation constant K_D = 0. 57 µM), the enthalpy change was $-7.84 \times 10^3 \pm 296$ kcal/mole and the entropy change was 1.84 ± 1.09 cal/(mole x °C). The stoichiometry of binding was 1.02 ± 0.04. In the Ca^{2+}-free buffer (1–2 mM EGTA), there was no binding of CaM to $NT_{60\text{-}120}$ (**Fig. 1C**). Thus, the binding of CaM to NSCaTE is Ca^{2+}-dependent, as previously shown for the whole NT[5] and as has been determined by FRET in transfected mammalian cells.[15]

Three a.a. are crucial for the function of the NSCaTE: W82, I86 and R90,[15] though the effect of the triple mutation has not been examined. We mutated all three residues to alanines (the "WIR" mutation; **Fig. 1E**) in the GST fusion protein (GST-$NT_{60\text{-}120WIR}$) and compared it with the wild type GST-$NT_{60\text{-}120WT}$. The WIR mutation abolished the interaction of CaM with the GST-$NT_{60\text{-}120WIR}$ in the presence of Ca^{2+} in the pull-down assay (**Fig. 1A**, middle). Accordingly, the ITC experiment showed there was no change in the release of heat and thus no interaction (**Fig. 1D**). These results confirm the crucial role of W82, I86 and R90 in CaM-α_{1C}-NT interaction and demonstrate that the triple WIR mutation fully abrogates CaM binding to NSCaTE.

Mutation of the CaM binding sequence does not change CDI significantly. Mutations in the IQ domain in the CT of α_{1C} abolish CDI,[4,6] but the role of CaM binding to NT in this channel is unclear. To address the specific contribution of the NT-CaM binding in α_{1C}, we explored the effect of the WIR mutation on the full channel expressed in *Xenopus* oocytes in the $\alpha_{1C} + \alpha_2/\delta + \beta_{2b}$ composition, with 40 mM Ba^{2+} or Ca^{2+} as permeant ions (I_{Ba} or I_{Ca}, respectively). In addition, we coexpressed CaM to ensure its presence at saturating doses; this did not change the inactivation parameters in either Ca^{2+} or Ba^{2+} (**Table 1**). A routine procedure to study the role of Ca^{2+} in Ca_V inactivation involves the use of Ba^{2+} or Ca^{2+} as permeant ions. This is believed to separate the two components of channel inactivation, the VDI and the CDI. The inactivation of I_{Ba} is considered to be only voltage-dependent (reviewed in ref. 16), while in Ca^{2+} both CDI and VDI operate (**Fig. 2A and B**).

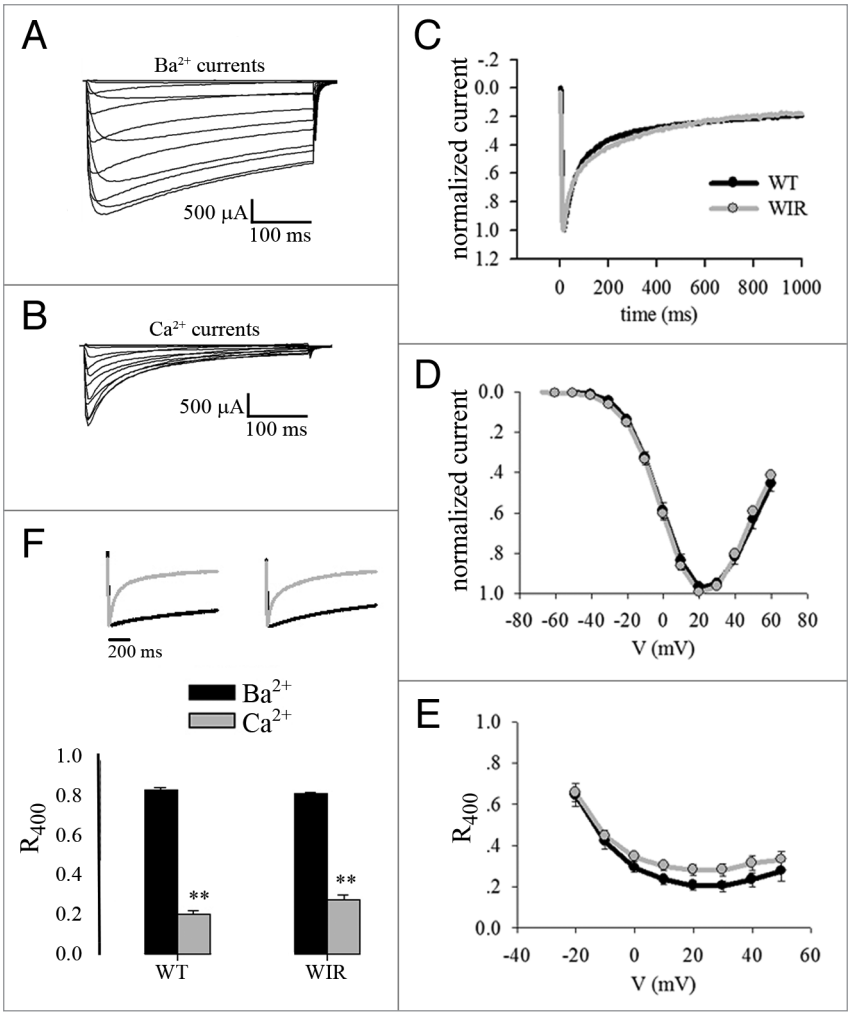

Figure 2. NT-CaM binding site does not play an important role in the inactivation of the channel. (A and B) Net I_{Ba} and I_{Ca} recorded in a representative oocyte with 400 ms depolarizing voltage steps from a holding potential of -80 mV. (C–E) Comparison of I_{Ca} of WT vs. WIR-α_{1C} co-expressed with CaM. (C) Normalized I_{Ca} in two representative cells at 20 mV. (D) Normalized IV curves averaged from 9 (WT) or 12 (WIR) oocytes. Data are presented as mean ± SEM. (E) Voltage dependence of r_{400}. Same cells as in 2. (F) R_{400} and f_{400} of Ca^{2+} and Ba^{2+} currents. Upper panel shows normalized I_{Ba} and I_{Ca} elicited by 1 s pulses in representative cells injected with WT (left) or WIR (right) channel. Bottom panel shows the corresponding average R_{400} values at +20 mV from 9 (WT) and 12 (WIR) oocytes. **p < 0.01 for Ca^{2+} vs. Ba^{2+} currents in eitehr WT or WIR oocytes.

Table 1. R_{400} at +20 mV in WT and WIR α_{1C}, with and without coexpression of CaM

Ion	Channel	R_{400}	S.E.M	n	p=	f_{400}	S.E.M	p=
Without CaM								
Ba^{2+}	WT	0.82	0.018	14	0.029			
	WIR	0.78	0.011	21				
Ca^{2+}	WT	0.22	0.02	8	0.039	0.60	0.018	<0.001
	WIR	0.27	0.04	7		0.50	0.011	
CaM coexpressed								
Ba^{2+}	WT	0.83	0.014	19	0.2			
	WIR	0.81	0.007	20				
Ca^{2+}	WT	0.20	0.02	9	0.012	0.63	0.007	<0.001
	WIR	0.28	0.02	12		0.53	0.014	

In all cases, α_{1C} was expressed with α_2/δ and β_{2b}.

To isolate the Ca^{2+}-dependent component of inactivation, we used a routine procedure that explores the differences between I_{Ca} and I_{Ba} and uses two parameters to analyze the results: R_{400} and f_{400}.[3,4] R_{400} reflects the total extent of inactivation within 400 ms; it is defined as $R_{400} = I_{400}/I_{max}$, i.e., the fraction of current remaining after 400 ms of depolarization (I_{400}) relative to peak current (I_{max}). f_{400}, defined as $R_{400}[I_{Ba}] - R_{400}[I_{Ca}]$ (at +20 mV), represents the difference in inactivated fractions in Ca^{2+} vs. Ba^{2+}. In other words, f_{400} is designed to provide an estimate of the isolated calcium-dependent component of inactivation ("net" CDI). Generally, there were no great differences between the inactivation of the WT and WIR channels in Ba^{2+} and in Ca^{2+} (**Fig. 2C–E**). Comparison of the f_{400} value between WT and WIR channel revealed a 10% reduction in WIR channel compared to the WT channel, either in the presence of absence of coexpressed CaM ($p < 0.01$, **Fig. 2F and Table 1**). The source of this difference appeared to derive from two components: a somewhat faster inactivation in Ba^{2+} (2–4% change) and a slightly slower inactivation in Ca^{2+} (5–8% change; **Fig. 2F and Table 1**).

In these experiments, the estimated maximal total concentration of BAPTA in the cytosol was ~2.5 mM (assuming a water volume of the oocyte of 0.5 µl and a homogenous distribution of BAPTA). To estimate the level of Ca^{2+} buffering attained in this way, we examined the CDI of neuronal N-type Ca^{2+} channels ($Ca_V2.2$), which have a high sensitivity to Ca^{2+} buffering. In mammalian cells, where the intracellular concentration of BAPTA can be strictly controlled in whole-cell recordings, CDI is almost fully abolished by 10 mM of intracellular BAPTA but not 0.5 mM EGTA.[10] The pore-forming α_{1B} subunit was coexpressed with β_{2a} subunit, which slows down the VDI,[17] to accentuate the differences in inactivation of Ba^{2+} and Ca^{2+} currents. In oocytes injected with the standard amount of BAPTA a weak CDI was still observed, with r_{400} of 0.87 ± 0.02 (n = 7) and f_{400} of 0.12 ± 0.01 at 20 mV (**Fig. 3**). With a 4-fold greater amount of BAPTA injected, $Ca_V2.2$ still showed the same CDI (r_{400}= 0.84 ± 0.01, and f_{400} = 0.13 ± 0.01) suggesting that, in the standard conditions, the Ca^{2+} buffering is already strong.

CaM is not a bridge between CT and NT. To examine whether CaM would form a "bridge" between NT and CT CaM-binding sites of α_{1C} in the presence of elevated Ca^{2+}, we examined the binding between GST-NT_{60-120} and an in vitro translated $CT_{1505-1671}$ (the C-terminal segment containing the binding site for CaM and the Ca-binding protein 1, CaBP1,[12,13]) in the presence or absence of CaM and Ca^{2+}. No interaction was observed between these parts of the channel with or without CaM and/or Ca^{2+} (**Fig. 4A**). The in vitro translated $CT_{1505-1671}$

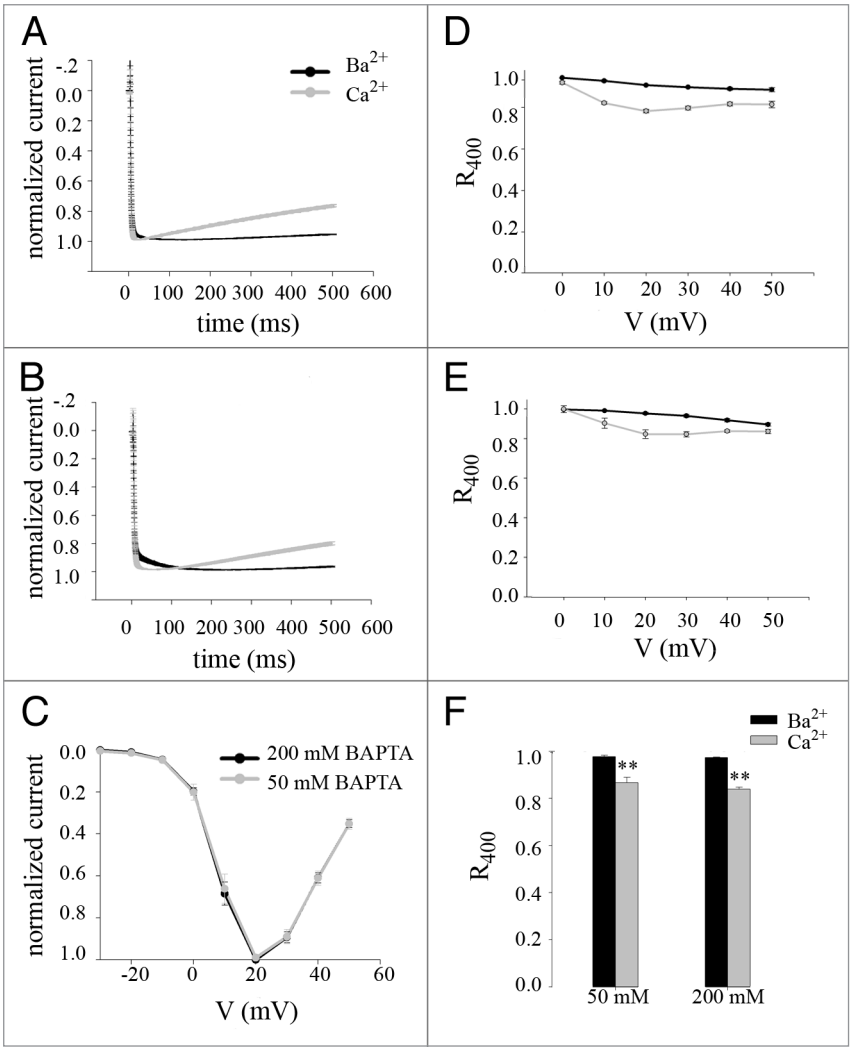

Figure 3. Only weak CDI is visible in N-type Ca^{2+} channel when Xenopus oocytes are injected with BAPTA. (A and B) Ca^{2+} and Ba^{2+} currents in oocytes injected with 30 nl of 200 mM BAPTA (A) or 50 mM BAPTA (B). The traces show currents recorded at 20 mV, averaged from 6 to 8 oocytes. Each point presents mean ± S.E.M. (C) Averaged I-V curves of I_{Ca} in oocytes injected with BAPTA. (D and E) R_{400} of I_{BA} and I_{Ca} in oocytes injected with 30 nl of 200 mM BAPTA (D) or 50 mM BAPTA (E). (F) Bar chart showing R_{400} measured at 20 mV in either Ba^{2+} or Ca^{2+} solution, in oocytes injected with the different doses of BAPTA. n = 6–8.

bound well the GST-fused CaBP1, as expected,[18] confirming the functionality of this protein (**Fig. 4B**).

Discussion

The main purpose of this study was to examine the role of the N-terminal CaM-binding site of α_{1C} in the Ca^{2+}-dependent inactivation process and to scrutinize the hypothesis that a direct connection between CT and NT, formed by the two lobes of CaM in the presence of Ca^{2+}, plays a role in CDI. Using ITC, we determined the K_D of the NT-binding site to CaM of 570 nM; this is in line with the 1.2 μM estimated by spectrofluorimetry.[15] In contrast to the CT, the binding of CaM to NT is strictly Ca^{2+}-dependent (reviewed in ref. 5 and **Fig. 1**). Note that our measurements of CaM affinity to the NT were done with the full-length CaM, whereas the CaM affinity measurements to the CT were done with the N-lobe or C-lobe alone.[12] It is possible that a separate measurement of the N-lobe and the C-lobe may reveal a different affinity.

The Ca^{2+} dependence of the NT-CaM interaction makes it a plausible candidate for a reversible, Ca^{2+}/CaM-dependent regulatory process such as CDI. However, NSCaTE, which appears to play a substantial role in CDI of $Ca_V1.3$,[15] does not appear to be strongly involved in the inactivation process in $Ca_V1.2$. The extent of inactivation with Ca^{2+} as the charge carrier was only slightly reduced (from 80% to ~75%, **Fig. 2**) in the WIR mutant channel, where all CaM binding to NT was eliminated (as confirmed by pull-down and ITC). Furthermore, the VDI was also changed by the WIR mutation by about the same extent, 5%, but in the opposite direction (weakened). Concerted though opposite changes in CDI and VDI caused by this mutation support the notion that these inactivation processes share common molecular determinants[2,19] and we propose that NSCaTE may be one of them.

Previous work has shown that the transfer of a proximal CT from α_{1C} to α_{1E} ($Ca_V2.3$) confers a strong local CDI upon the latter, despite the lack of NSCaTE motif in the α_{1E} NT, consistent with our findings.[20] However, because of the strong Ca^{2+} buffering used in that study,[20] a role for NT in conferring a component of CDI that is dependent on "global" Ca^{2+} (as it happens in $Ca_V1.3$,[15]) can not be excluded. Also in our work, we cannot definitely rule out the possibility that we have overlooked a component of CDI caused by an intracellular Ca^{2+} increase beyond the channel's nano-domain, which might be NSCaTE-dependent, because of our use of the fast Ca^{2+} chelator BAPTA for intracellular Ca^{2+} buffering. The persistence of Ca^{2+}-activated Cl^- currents inherent to the oocytes under mild Ca^{2+} chelation (e.g., with EGTA) precluded the study of this particular aspect of CDI. However, the CDI in $Ca_V1.2$ is almost fully operated by the nano-domain Ca^{2+} entering the cell via the channel itself, which is insensitive to BAPTA; a component relying on intracellular Ca^{2+} is minor or even negligible. Thus, the maximal extent of inactivation within 400 ms with Ca^{2+} as charge carrier in our experiments was 80% (r_{400} = 0.2), identical to that measured in α_{1C} with high BAPTA buffering in mammalian cells or oocytes.[3,4] Moreover, 80% inactivation is exactly the maximal inactivation attainable in $Ca_V1.2$ channels at high $[Ca]_{in}$ of 200 μM, without any Ca^{2+} buffering.[21] We conclude that, under conditions close to those occurring in intact cells, the NSCaTE plays only a minor role in inactivation caused by Ca^{2+} entry via $Ca_V1.2$ due to membrane depolarization. The NT-Ca^{2+} dependent-CaM binding site may have another role in channel modulation, yet to be discovered. Since Ca^{2+} entry via the $Ca_V1.2$ in the cardiomyocyte causes the release of Ca^{2+} from the sarcoplasmic reticulum, there is a possibility that the NSCaTE

is influenced by this Ca^{2+}, which can not be measured with the experimental tools used in this work.

Potentially, the N-lobe of CaM could become available to bind the NSCaTE if detached from its binding site in the IQ domain, while the C-lobe is anchored at the IQ domain.[15] On the other hand, the K_D of binding affinity of a complete CaM to the IQ domain should be below 2 nM, given the high affinities of separately bound N and C lobes.[12] In view of the much lower affinity of CaM-NSCaTE binding (0.6 μM; **Fig. 1**), it is unlikely that the CaM N-lobe detaches from the IQ site to NSCaTE, bridging the NT and CT domains. Indeed, our results do not support a model in which CaM forms a direct "bridge" between the N- and C-terminal CaM binding sites. However, more sophisticated models involving regulation of CDI by triple NT/CT/Ca-CaM interactions should be considered. The inhibitory modules in NT and CT are at their distal ends and do not overlap with CaM binding sites. Yet, functional data suggest that they interact, directly or via a third party.[5,22] Additional binding determinants on both CT and NT may exist. In the context of such interactions between the full-length CT and NT (if they exist), Ca^{2+}-dependent CaM binding to the specific sites in NT and CT could alter the conformation of the whole NT-CT scaffold to affect the inactivation process. Alternatively, a role for NSCaTE in binding an additional (second) CaM following Ca^{2+} entry should also be considered.

Materials and Methods

Expression system, DNAs and RNAs. Maintenance of the female frogs (*Xenopus laevis*), preparation of oocytes and in vitro RNA synthesis were as described.[23] Oocytes were injected with RNAs 3–5 days before the experiment with 2.5–5 ng of RNA of rabbit heart α_{1C} (X15539), β_{2b} (L06110), and skeletal muscle $\alpha_2\delta$-1 (P13806).[23] The cDNAs of the channel segments were inserted into pMXT vector (for in vitro translated proteins) and pGEX-4T1 (for GST-fusion proteins GST-CaBP1-S (human Ca-binding protein 1, short isoform[18]), GST-NT_{60-120} and GST-$NT_{60-120WIR}$). The WIR mutations in α_{1C} and its segments were constructed by standard PCR methods. Human CaM cDNA was inserted into pET-15b (Novagen). For expression of NT_{60-120}, pET-Duet-1 (Novagen) was modified to encode a 8xHisTag and a tobacco etch mosaic virus (TEV) protease cleavage site upstream and in frame with residues 60–120 of rabbit $Ca_V1.2$ inserted into multiple cloning site-1 (MCS1). Human CaM cDNA was inserted into MCS2.

Protein purification and pull-down assays. All proteins were expressed in *E. coli* Tuner (DE3) Codon Plus or BL21 cells grown in standard media at 37° or 16°C after induction with IPTG. Cell lysis was done by microfluidizer (Microfluidics, Newton, MA, USA). The GST-fusion proteins were prepared using standard protocols[5] and purified on ÄKTAprime (GE Healthcare, USA), followed by gel-filtration chromatography on Superdex 200 column in the experiment buffer. For CaM purification, the procedure described by Hayashi et al.[24] was used with slight modifications. After lysis, the soluble fraction was heated to 90°C for 5 minutes, then centrifuged prior to loading on the Phenyl-sepharose column. Subsequently, an additional

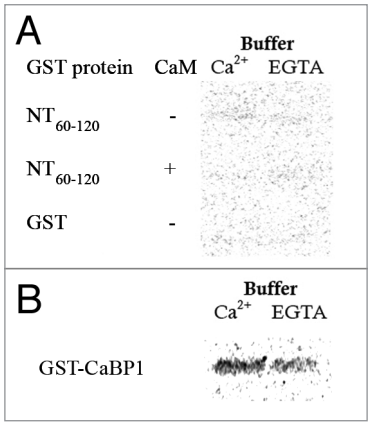

Figure 4. CaM in not a bridge between CT and NT. (A) Interaction on in vitro translated $CT_{1505-1671}$ with GST-NT_{60-120} in the presence of 1 mM Ca^{2+} or 1 mM EGTA, with or without the addition of 3 μg of purified CaM. The experiment was done in binding buffer with 0.5% CHAPS. This is a representative experiment out of two. The bands are the autoradiographic images of $CT_{1505-1671}$. (B) Interaction of GST-fused CaBP1 with in vitro translated $CT_{1505-1671}$. Same experimental paradigm as in (A) was used.

Q-Sepharose chromatography step was added where the protein was eluted by a linear salt gradient (0–0.5 M NaCl). For NT_{60-120} purification, cells were lysed in a solution of Ni^{2+} column buffer (50 mM Tris pH 7.5, 200 mM NaCl, 20% glycerol, 5 mM $CaCl_2$) supplemented by 0.1% Triton X 100 and 2 mM phenylmethylsulphonyl fluoride. The soluble fraction was loaded onto a Ni^{2+} chelate column and the NT_{60-120}/CaM complex was eluted with imidazole. Elution fractions were analyzed by SDS-PAGE. Pooled protein fractions were proteolyses with TEV to remove the polyhistidine tag and dialyzed overnight against Ni^{2+} column buffer, with 2.5 mM EGTA replacing $CaCl_2$, to enable separation of CaM from NT_{60-120}. The dialysate was diluted four fold, loaded onto a SP-Sepharose column where the CaM-free NT_{60-120} was eluted by a linear salt gradient (50–620 mM NaCl). Pure NT_{60-120} was collected from a single peak on a Superdex-200 Hi-prep gel filtration column (GE Healthcare) in 20 mM Tris pH 7.5, 120 mM NaCl.

Protein concentrations were determined at λ = 280 nm using extinction coefficients calculated by amino acid analysis (ProtParam tool, http://expasy.org/tools/protparam.html). Pull-down experiments were performed with glutathione affinity beads as described[5] using binding buffer with 1 mM Ca^{2+} or 1 mM EGTA (150 mM KCl, 50 mM Tris, 5 mM $MgCl_2$ and 1 mM $CaCl_2$ or EGTA, pH = 7.0).

Isothermal titration calorimetry (ITC). Titrations were performed using a VP-ITC calorimeter (MicroCal, Northampton, MA) at 20°C in a buffer containing 20 mM Tris and 120 mM NaCl (pH 7.5) with the addition of 1–2 mM $CaCl_2$ or 1–2 mM EGTA. The titration of binding of CaM to NT_{60-120} was done by injection of 5–10 μl CaM into the sample cell containing 1.4 ml of NT_{60-120}. Each injection was carried out over a 12–20 s period, with a 120–240 s delay between injections, sufficient for the baseline to be reestablished. The cell was constantly rotated. The data obtained from ITC were analyzed using the Origin software package for ITC (Microcal). The data were fit using a one binding site model.

Electrophysiology and statistical analysis. Whole cell currents were recorded using the Gene Clamp 500 amplifier (Axon Instruments, Foster City, CA) using the two-electrode voltage clamp. 25–30 nl of 50 mM BAPTA (Ca^{2+} chelator) were routinely injected into the oocytes 0.5–3 hours before the measurement of currents. This procedure usually blocked the endogenous Ca^{2+}-dependent Cl^- currents; cells with residual Cl^- currents (distinguished by long-lasting inward tails at -80 mV) were excluded from analysis. The high-Ba^{2+} (or high-Ca^{2+} solution) contained 40 mM $Ba(OH)_2$ or 40 mM $Ca(NO_3)_2$, respectively, 50 mM NaOH, 2 mM KOH and 5 mM HEPES, titrated to pH 7.5 with methanesulfonic acid. Current-voltage (I-V) relations were measured with 400 or 1,000 ms pulses from holding potential of -80 mV to -70 mV to +70 mV in 10 mV steps. In each cell, the net I_{Ba} and I_{Ca} were obtained by subtraction of the residual currents recorded with the same protocols after blocking Ca^{2+} channel currents with 200–400 μM Cd^{2+}. Stimulation and data analysis were performed using pCLAMP software (Axon Instruments), graphs and statistical analysis with SigmaPlot (SPSS , Inc., Chicago, IL). Comparison between several groups was done using one-way analysis of variance (ANOVA) followed by Tukey's test, using the SigmaStat software (SPSS Corp.,).

Acknowledgements

This work was supported by the Israel-USA Binational Science Foundation (grant 2005340) to Nathan Dascal and a Israel Science Foundation grant (1201/04) to Joel A. Hirsch. We thank Dr. Amy Lee (Univ. of Iowa) for critical reading and helpful suggestions, Oshik Segev for help with ITC analysis, and Nataly Kanevsky for producing some of the mutations in α_{1C}.

References

1. Catterall WA. Structure and regulation of voltage-gated Ca^{2+} channels. Annu Rev Cell Dev Biol 2000; 16:521-55.
2. Findeisen F, Minor DL Jr. Disruption of the IS6-AID linker affects voltage-gated calcium channel inactivation and facilitation. J Gen Physiol 2009; 133:327-43.
3. Peterson BZ, DeMaria CD, Adelman JP, Yue DT. Calmodulin is the Ca^{2+} sensor for Ca^{2+}-dependent inactivation of L-type calcium channels. Neuron 1999; 22:549-58.
4. Zuhlke RD, Pitt GS, Deisseroth K, Tsien RW, Reuter H. Calmodulin supports both inactivation and facilitation of L-type calcium channels. Nature 1999; 399:159-62.
5. Ivanina T, Blumenstein Y, Shistik E, Barzilai R, Dascal N. Modulation of L-type Ca^{2+} channels by Gβγ and calmodulin via interactions with N- and C-termini of α_{1C}. J Biol Chem 2000; 275:39846-54.
6. Qin N, Olcese R, Bransby M, Lin T, Birnbaumer L. Ca^{2+}-induced inhibition of the cardiac Ca^{2+} channel depends on calmodulin. Proc Natl Acad Sci USA 1999; 96:2435-8.
7. Calin-Jageman I, Lee A. Ca_V1 L-type Ca^{2+} channel signaling complexes in neurons. J Neurochem 2008; 105:573-83.
8. Lee A, et al. Ca^{2+}/calmodulin binds to and modulates P/Q-type calcium channels. Nature 1999; 399:155-9.
9. Falke JJ, Drake SK, Hazard AL, Peersen OB. Molecular tuning of ion binding to calcium signaling proteins. Q Rev Biophys 1994; 27:219-90.
10. Liang H, et al. Unified mechanisms of Ca^{2+} regulation across the Ca^{2+} channel family. Neuron 2003; 39:951-60.
11. Tang W, et al. Apocalmodulin and Ca^{2+}calmodulin-binding sites on the $Ca_V1.2$ channel. Biophys J 2003; 85:1538-47.
12. Van Petegem F, Chatelain FC, Minor DL Jr. Insights into voltage-gated calcium channel regulation from the structure of the $Ca_V1.2$ IQ domain-Ca^{2+}/calmodulin complex. Nat Struct Mol Biol 2005; 12:1108-15.
13. Erickson MG, Liang H, Mori MX, Yue DT. FRET two-hybrid mapping reveals function and location of L-type Ca^{2+} channel CaM preassociation. Neuron 2003; 39:97-107.
14. Kim J, Ghosh S, Nunziato DA, Pitt GS. Identification of the components controlling inactivation of voltage-gated Ca^{2+} channels. Neuron 2004; 41:745-54.
15. Dick IE, et al. A modular switch for spatial Ca^{2+} selectivity in the calmodulin regulation of Ca_v channels. Nature 2008; 451:830-4.
16. Babich O, Matveev V, Harris AL, Shirokov R. Ca^{2+}-dependent inactivation of $Ca_V1.2$ channels prevents Gd^{3+} block: does Ca^{2+} block the pore of inactivated channels? J Gen Physiol 2007; 129:477-83.
17. Yasuda T, et al. Auxiliary subunit regulation of high-voltage activated calcium channels expressed in mammalian cells. Eur J Neurosci 2004; 20:1-13.
18. Zhou H, et al. Ca^{2+}-binding protein-1 facilitates and forms a postsynaptic complex with $Ca_V1.2$ (L-type) Ca^{2+} channels. J Neurosci 2004; 24:4698-708.
19. Cens T, Restituito S, Galas S, Charnet P. Voltage and calcium use the same molecular determinants to inactivate calcium channels. J Biol Chem 1999; 274:5483-90.
20. de Leon M, et al. Essential Ca^{2+}-binding motif for Ca^{2+}-sensitive inactivation of L-type Ca^{2+} channels. Science 1995; 270:1502-6.
21. Lacinova L, Hofmann F. Ca^{2+}- and voltage-dependent inactivation of the expressed L-type $Ca_V1.2$ calcium channel. Archives of Biochemistry and Biophysics 2005; 437:42-50.
22. Kobrinsky E, et al. Differential role of the α_{1C} subunit tails in regulation of the $Ca_V1.2$ channel by membrane potential, β subunits and Ca^{2+} ions. J Biol Chem 2005; 280:12474-85.
23. Shistik E, Ivanina T, Blumenstein Y, Dascal N. Crucial role of N terminus in function of cardiac L-type Ca^{2+} channel and its modulation by protein kinase C. J Biol Chem 1998; 273:17901-9.
24. Hayashi N, Matsubara M, Takasaki A, Titani K, Taniguchi H. An expression system of rat calmodulin using T7 phage promoter in *Escherichia coli*. Protein Expr Purif 1998; 12:25-8.